

1 Miniaturized NIR and MIR spectroscopy for insect lipid characterization

2
3 C. Mendez-Sanchez¹, M. K. Ranasinghe¹, C. Güell¹, M. Ferrando¹, J.C. Domingo², and S. de
4 Lamo Castellvi^{1,3,*}

5 ¹Universitat Rovira i Virgili, Departament d'Enginyeria Química, Av. Països Catalans 26, Campus
6 Sescelades, 43007 Tarragona, Spain; ²Department of Biochemistry and Molecular Biology,
7 University of Barcelona, Barcelona, Spain; ³Department of Food Science and Technology, The
8 Ohio State University Columbus, OH 43210-1007, USA

9 *Corresponding autor. Email: silvia.delamo@urv.cat

10 **Running header:** Insect lipid characterization by MIR and NIR

11 12 RESEARCH ARTICLE

13 Abstract

14 The main objective of this research was to evaluate the performance of portable FT-MIR (4000 to
15 630 cm⁻¹) and handheld FT-NIR (7400 to 4000 cm⁻¹) spectrometers, combined with partial least
16 squares regression (PLSR) multivariate analysis. This method was used to predict the percentage
17 of insect lipids added to mixtures of vegetable and seed oils, as well as to profile the fatty acid
18 composition in the lipid fractions of *Locusta migratoria* and *Acheta domesticus* mixed with these
19 oils. Insect lipids from *L. migratoria* and *A. domesticus* were extracted from their powdered forms
20 using organic solvent extraction and then mixed with five edible oils (olive, sunflower, avocado,
21 almond, and linseed) at concentration ratios ranging from 0% to 100% (n = 140). The fatty acid
22 (FA) profile of the samples was determined using the fatty acid methyl ester (FAME) method.
23 PLSR was used to develop algorithms for predicting insect lipid content in mixtures and FA
24 composition. The PLSR model for predicting the percentage of insect lipids in mixtures with
25 vegetable and seed oils demonstrated good linearity, with high correlation (R_{CV} = 0.99), low
26 standard errors of cross-validation (SE_{CV} ≤ 2.21%) and prediction (SE_P ≤ 2.32%), and high
27 predictive performance as indicated by the ratio of prediction to deviation (RPD ≥ 9.23). The
28 percentage of myristic, palmitic, stearic, oleic, linoleic, and α-linolenic fatty acid as well as the
29 content of saturated (SFA), monounsaturated (MUFA), and polyunsaturated (PUFA) were
30 accurately predicted with values of SE_{CV} ≤ 4.64% and an R_{CV} ≥ 0.88. However, the FT-MIR
31 spectrometer tested showed superior performance in predicting fatty acids and SFA, MUFA, PUFA
32 reaching values of 0.99 in coefficient of correlation (RP) and 0.66% in standard error in prediction
33 (SE_P).

34 **Key words:** insect lipids, *L. migratoria*, *A. domesticus*, mid-infrared spectroscopy, near-infrared
35 spectroscopy.

36 **Conflicts of interest.** The authors declare no conflict of interest.

37 **Funding statement.** This project was financially supported by the fundings from Ministerio de
38 Economía y Competitividad PGC 2018-097095-B-I00. C. Mendez reports support Diputació de
39 Tarragona and the Universitat Rovira i Virgili (2020PMF-PIPF-30).

40

41 1. Introduction

42 Lipids, along with proteins, are primary components of insects. Recent research has characterized
43 numerous insect species, revealing that lipid composition and content may be influenced by factors
44 such as insect species, life stage, diet, and fat extraction method (Arrese and Soulages, 2010;
45 Laroche *et al.*, 2019; Oonincx and Van Der Poel, 2011). Insects accumulate essential nutrients and
46 energy as lipids to support survival through metamorphosis or other non-feeding activities (Dossey
47 *et al.*, 2016). Insect lipids have been evaluated as alternative ingredients for various applications,
48 including bakery products, spreads, frying oils, food-grade lubricants, and emulsions, with
49 promising results (Tzompa-Sosa and Fogliano, 2017). Additionally, potential applications in the
50 cosmetic, therapeutic, and industrial sectors have been proposed (Aguilar, 2021; Franco *et al.*,
51 2021). The quality and functionality of these lipids depend on their fatty acid (FA) profile. Notably,
52 the primary FA in insects includes palmitic acid (C16:0), stearic acid (C18:0), oleic acid (C18:1n9)
53 and linoleic acid (C18:2n6) (Rumpold and Schlüter, 2013). While palmitic acid can be produced
54 endogenously, dietary intake may still be required (Carta *et al.*, 2017). Palmitic and stearic acids
55 are of interest for biodiesel production due to their high calorific value and viscosity (Manzano-
56 Agugliaro *et al.*, 2012). Oleic acid, a monounsaturated FA, is associated with health effects such
57 as anti-inflammatory effects and is utilized in cosmetics for its skin penetration properties (Rabasco
58 Alvarez and González Rodríguez, 2000; Sales-Campos *et al.*, 2013). Linoleic acid, an essential
59 omega-6 FA, is linked to health benefits and participates in omega-3 metabolic pathways (Viola
60 and Viola, 2009).

61 Several studies have demonstrated that insect lipids can effectively replace vegetable and seed oils
62 in food formulations. For example, insect lipids from *Schistocerca gregaria* and *Ruspolia differens*
63 were successfully used in cookies, with consumer preference favoring those made with *R. differens*
64 and sesame oil (Cheseto *et al.*, 2020). Additionally, *Hermetia illucens* larvae fat was able to
65 substitute up to 25% of butter in bakery products without altering taste (Delicato *et al.*, 2020), and
66 *Tenebrio molitor* oil (crude or deodorized) was shown to replace partially replace peanut and
67 rapeseed oils in crackers and hummus without negatively affecting consumer acceptance (Tzompa-
68 Sosa and *et al.*, 2021a, 2021b).

69 FA are commonly analyzed using gas chromatography (GC), a labor-intensive method, that
70 requires complex sample pretreatment, and results in sample destruction. Infrared (IR)
71 spectroscopy, when combined with pattern recognition analysis, has been proposed as an
72 alternative technique for predicting FA percentages (Aykas *et al.*, 2020; Salas-Valerio *et al.*, 2022;
73 Yao *et al.*, 2020). Benchtop Fourier-transform mid-infrared (FT-MIR) spectrometers have been also
74 employed to study oxidative stability by quantifying peroxide and anisidine values (Guillén and
75 Cabo, 2002), determine omega-6 and omega-3 amount and ratios (Olsen *et al.*, 2008), and
76 authenticate extra virgin olive oil (Lerma-García *et al.*, 2010). Similarly, benchtop near-infrared
77 (NIR) equipment has been used to assess quality parameters such as acidity, volatile matter,
78 peroxide index, and insoluble impurities in olive oil (Garrido-Varo *et al.*, 2017) and other edible
79 oils (Armenta *et al.*, 2007). Recent advancements in IR spectroscopy have enabled the
80 miniaturization of equipment, allowing for in situ analysis (Cebi *et al.*, 2023; Rodríguez-Saona *et al.*,
81 2016). The integration of technologies such as Linear Variable Filters (LVF) and micro-electro-
82 mechanical systems (MEMS) has resulted in the development of palm-sized NIR spectrometers
83 (Yan and Siesler, 2021). Portable NIR equipment, such as the NeoSpectra Scanner, which operates
84 in the 7400 to 4000 cm^{-1} range and incorporates MEMS advancements, has been used to predict
85 trans-fat content in edible oils (Birkel and Rodríguez-Saona, 2011). The MicroNIR spectrometer,

86 utilizing an LVF wavelength selector and collecting spectra from 11000 to 6000 cm^{-1} , has been
87 evaluated for quantifying olive oil in various vegetable oils (Borghi *et al.*, 2020). Portable MIR
88 devices, such as those based on the Michelson interferometer, have also been applied to lipid
89 analysis. For instance, spectral data obtained using a portable Agilent Cary 630 has been utilized
90 to identify the type of vegetable oil used for frying chips (Aykas and Rodriguez-Saona, 2016) and
91 determine fatty acid composition in frying oils and fish oil supplements (Aykas and Rodriguez-
92 Saona, 2016; Plans *et al.*, 2015). The handheld TruDefender has been employed to create prediction
93 models for quantifying major fatty acids in butter and margarine (Salas-Valerio *et al.*, 2022).
94 Additionally, the Bruker-Alpha spectrometer has been tested for quantifying free fatty acids in olive
95 oil (Tarhan *et al.*, 2017) and measuring refractive index, peroxide value, and total phenolic content
96 in pomegranate kernel oil (Okere *et al.*, 2022).

97 The aim of this study was to assess the potential of miniaturized FT-MIR and FT-NIR devices,
98 combined with PLSR, to predict the amount of *Locusta migratoria* and *Acheta domesticus* lipids
99 mixed with sunflower, almond, olive, avocado, and linseed oils. Additionally, the lipid samples
100 were analyzed to predict the percentages of saturated, monounsaturated, and polyunsaturated fatty
101 acids, as well as the specific fatty acid profiles, including myristic, palmitic, stearic, oleic, linoleic,
102 and α -linolenic acids.

103

104 **2. Material and Methods**

105 *Lipid extraction procedure*

106 Lipids from *A. domesticus* (AD) and *L. migratoria* (LM) powders supplied by Delibugs (Lelystad,
107 Netherlands, two batches from the same lot) were extracted using the organic solvent extraction
108 method described following the procedure of Wang *et al.* (2021). First, the insect powder was
109 mixed with 2-methyltetrahydrofuran (2- MTHF) (Scharlab S.L., Barcelona, Spain) at 1/5 (w/w)
110 ratio and stirred at 300 rpm for 1 h at room temperature. The mixture was allowed to fully separate
111 in two phases. The upper phase, containing the lipid fraction, was collected, while the lower phase,
112 with the partially defatted insect powder, underwent two additional defatting cycles using more 2-
113 MTHF. The collected upper phases were combined in a round-bottom flask, and the 2-MTHF was
114 evaporated (SBS-RV-2000, Steinberg, Germany) at 400 mbar and 65 °C and the lipid fraction was
115 recovered. The insect lipids were stored at 4 °C under a nitrogen atmosphere and protected from
116 ambient light until further use.

117 *Sample preparation*

118 Samples were prepared by mixing lipid fractions from *A. domesticus* and *L. migratoria* with two
119 batches from the same lot of sunflower oil (SF) (Borges, Tarragona, Spain), extra virgin olive oil
120 (OL) (Aceites molisur, Málaga, Spain), avocado oil (AV) (Perseus Foods, Guecho, Spain), linseed
121 oil (LI) (Ecoveritas S.A., Barcelona, Spain) and almond oil (AL) (Ecoveritas S.A., Barcelona,
122 Spain) (supplementary Table S1 and Table S2). A total of 140 samples, each with 50 mL, were
123 prepared by mixing one insect species with a vegetable or seed oil in increasing ratios of 10% by
124 weight, ranging from 0% to 100% of the final weight.

125 *Determination of fatty acids profile*

126 The fatty acids profile from all the vegetables and seed oils and insect lipid extracts used in this
127 study were obtained by Gas Chromatography-Mass Spectroscopy (GS-MS). Fatty acid methyl
128 esters (FAME) were prepared following the method Lepage and Roy (1986) by transesterification
129 of the fatty acids present in the samples by addition of methanol-hexane (4:1, v/v). Then, 200 μL
130 of acetyl chloride was added and heated at 100 °C for 1h. After that, potassium carbonate was
131 added into the tube and centrifuged. The upper phase, which contains the FAME, was collected
132 and analyzed. 1 μL of the sample was analyzed to determine the fatty acid composition with
133 Shimadzu GCMS- QP2010 Plus gas chromatograph/mass spectrometer (Shimadzu, Kyoto, Japan),
134 equipped with a split/splitless injector, a Shimadzu AOC-20i autoinjector, a Shimadzu AOC-20s
135 autosampler and a Suprawax-280 (Teknokroma, 15m length x 0.10mm internal diameter x 0.10 μm
136 film thickness) column. The oven's settings were as follows: 130 °C for 0.25 min, followed by a
137 ramp of 35 °C/min to 200 °C, 225 °C (8 °C/min) for 3.2 min, and 80 °C/min to 245 °C for 2.75
138 min. By comparing the elution times of the reference FAME mixture (GLC-744 Nu-Chek Prep.
139 Inc., Elysian, Minnesota, USA), the fatty acids present in the samples were identified. The
140 proportion of each fatty acid in the total is shown by the values of the fatty acid profile. Every
141 sample was analyzed twice. The percentage of saturated fatty acids (SFA) was determined as the
142 sum of C12:0, C14:0, C16:0, C18:0, and C20:0; the monounsaturated fatty acids (MUFA) as the
143 sum of C16:1n7, C16:1n9, C18:1n9, C18:1n7, and C20:1n9; the polyunsaturated fatty acids
144 (PUFA) percentage as the sum of C18:2n6, and C18:3n3; and the unsaturated fatty acids (UFA)
145 percentage as the sum of MUFA and PUFA. The total amount of omega-6 (n6) is composed by
146 C18:2n6, and the total amount of omega-3 (n3) is composed by C18:3n3.

147 *Infrared analysis*

148 The portable Agilent Cary 630 (Agilent Technologies Inc., Santa Clara, CA) equipped with a
149 deuterated triglycine sulfate detector and single-bound attenuated total reflectance (ATR) diamond
150 crystal accessory was used to acquire FT-MIR spectral data. The spectra were collected with an 8
151 cm^{-1} resolution, to enhance the signal-to-noise ratio 128 interferograms were coadded in the range
152 of 4000 to 650 cm^{-1} . The samples were held at 45 °C and 0,8 μL of sample was placed on the ATR
153 crystal to collect the spectrum. Each sample was measured five times.

154 The FT-NIR spectral data measurements were collected using Neospectra scanner (Si-Ware
155 Systems, Cairo, Egypt) equipped with a single uncooled InGaAs photodetector and a monolithic
156 MEMS-based Michelson interferometer chip. 350 μL of oil mixture at 45 °C were placed in the
157 vials for analysis liquids (Si-Ware Systems, Inc., Cairo, Egypt) and covered with a reflectance
158 accessory. Spectra were recorded using Neospectra Collect App (Si-Ware Systems) within the
159 range of 7400 to 4000 cm^{-1} during 10 s. All the samples were analyzed in duplicate, collecting the
160 background signal between each measurement.

161 *Multivariate data analysis*

162 Pirouette 4.5 (Infometrix Inc., Washington, DC, USA) was used for the multivariate analysis. The
163 NIR spectra were treated by Standard Normal Variate (SNV) and a second Savitzky–Golay
164 derivative (9-point window size). MIR data were transformed by normalization followed by the
165 second derivative transformation (17-point window size). All the data were mean-centered before
166 the analysis. Principal Component Analysis (PCA) is an unsupervised pattern recognition
167 algorithm, it was performed to study the main differences between the samples included in this
168 study. Partial least squares regression (PLSR) models were developed to quantify insect lipids
169 content and the FA profile based on the reference values obtained by GC-MS. The dataset was

170 divided into a calibration set (n=107) for model training and a validation set (n=40) for performance
171 assessment using the Kennard-Stone algorithm. PLSR models were generated based on results
172 obtained by GC-MS. Internal cross-validation (leave-one-out) was performed during the
173 calibration to evaluate model performance. The number of factors was determined by the minimum
174 standard error of cross-validation (SE_{CV}) and the correlation coefficient of cross-validation (R_{CV})
175 values to avoid overfitting and underfitting. The best PLSR models were validated by predicting
176 the insect lipid content and FA profile from the validation sample set. The standard error of
177 prediction (SE_P), the correlation coefficient of prediction (R_P), and the ratio of performance to
178 deviation (RPD) were calculated to determine regression model performance.

179 3. Results and Discussion

180 *FTIR analysis and chemometric approach*

181 Figure 1. shows a representative *A. domesticus* (AD), *L. migratoria* (LM), sunflower (SF), olive
182 (OL), avocado (AV), linseed (LI), and almond (AL) oils acquired by FT-MIR. The spectra
183 presented absorption bands at 3007 cm^{-1} linked to $=\text{C}-\text{H}$ cis stretching and bands at 2955, 2922,
184 and 2851 cm^{-1} corresponding to $\text{C}-\text{H}$ symmetric and asymmetric stretching vibrations (Aykas and
185 Rodriguez-Saona, 2016). The band at 1744 cm^{-1} was associated with the carboxyl group ($\text{C}=\text{O}$) of
186 the esters stretching vibration, characteristic of the lipids (Salas-Valerio *et al.*, 2022). The signal at
187 1647 cm^{-1} was related to $\text{C}=\text{C}$ stretching of cis double bonds; and the following bands at 1457 and
188 1379 cm^{-1} , to bending vibration of $\text{C}-\text{H}$ from CH_2 and CH_3 group respectively (Aykas *et al.*, 2020),
189 and the band at 723 cm^{-1} corresponds to cis $\text{C}-\text{H}$ (Aykas and Rodriguez-Saona, 2016). The FT-NIR
190 spectra of the insects and vegetable and seeds oil in Figure 2 showed substantial variations in five
191 bands at 5800, 5678 4670, 4330, and 4234 cm^{-1} . The IR bands at 5800, 5678 cm^{-1} were linked to
192 $\text{C}-\text{H}$ from CH_2 stretching first overtone (Benes *et al.*, 2022), and the band at 4670 cm^{-1} , was
193 associated with vibrations arising from $\text{C}-\text{H}$ groups from double bonds (Garrido-Varo *et al.*, 2015).
194 The bands ranged from 4384 to 4084 cm^{-1} were related to combination modes of $\text{C}-\text{H}$ (Ozaki *et al.*,
195 2018). The spectra showed absorption bands at similar wavenumbers to those previously reported
196 by the same device with other lipidic samples, such as butter or vegetable oils (Salas-Valerio *et al.*,
197 2022; Yao *et al.*, 2020).

198 *Pattern recognition*

199 In this study, Principal Component Analysis (PCA) was performed as an exploratory tool to detect
200 patterns between the pure oils and mixed with *A. domesticus* and *L. migratoria* lipids. Figures 3
201 and 4 show the score plots of the resulting PCA obtained from the FT-MIR and FT-NIR input,
202 respectively. The type of vegetable or seed oil used and its percentage in the mixture were indicated
203 on the sample labels. The first principal component consistently discriminated the percentage of
204 insect lipids from vegetable and seed oils, while the second principal component differentiated the
205 various types of oils. The large spread of samples in the class projection plot showed the variability
206 among the selected oils. The formation of clusters observed in this study was also noted by
207 researchers combining insect powders with wheat flour (Benes *et al.*, 2022). In MIR analyses PC1
208 and PC2 explained 98.8 % and 97.7% of the variance for *A. domesticus* and *L. migratoria* samples,
209 respectively. The loadings provided information about the variables that contributed most
210 significantly to the discrimination. The bands of interest were centered in the lipid region. The most
211 important bands identified by PCA were 2918, 2881, 2851, 1770, 1744, 1714, and 1155 cm^{-1} . The
212 bands 2918, 2881 and 2851 cm^{-1} were related to the asymmetric stretching vibration of $\text{C}-\text{H}$ from
213 CH_2 groups; the bands at 1770, 1744, and 1714 cm^{-1} were associated with the stretching vibration

214 of C=O from the fatty acids functional group; and the signal from the stretching vibration of the C-
 215 O ester groups was observed at 1155 cm⁻¹ (Aykas and Rodriguez-Saona, 2016; Lerma-García *et*
 216 *al.*, 2010). Variations in signal at these bands resulted from differences in the fatty acid chains of
 217 the oils particularly among the vegetable oils, as most of the bands were represented in PC1. These
 218 differences were attributed to variations in chain length and degree of unsaturation. Similar bands
 219 were reported by other authors in the discrimination of extra virgin olive, virgin olive, olive, and
 220 adulterated olive oils (Aykas *et al.*, 2020). A similar approach was considered in PCA analysis using
 221 FT-NIR spectra, the two main PC explained 98.3% of *A. domesticus* and 98.2% of *L. migratoria*
 222 of the variance. The NIR bands at 5923, 5868, 5827, 5787, 5759, 4411, 4343, 4221, and 4112 cm⁻¹
 223 explained most of the variance in the PCA. The bands between 5923 to 5759 cm⁻¹ are associated
 224 with the first overtone of C-H stretching of CH₃ and carbons double bonds, the ones between 4411
 225 and 4112 cm⁻¹ are mainly related to C-H from CH₃ and stretching of CH₂ bonds, both from fatty
 226 acids chains (Christy *et al.*, 2004). The wavenumber absorptions described in the loadings were
 227 like those previously identified by other researchers in the authentication potato chip frying oil,
 228 they also found relevant the bands from 5900 to 5600 cm⁻¹ authors (Yao *et al.*, 2020). Similar to
 229 our findings with FT-MIR spectral data, the primary differences were linked to the vegetable oils
 230 and their compositional variations.

231 *PLSR models to predict the percentage of insect lipid content*

232 PLSR calibration models created with FT-MIR and FT-NIR spectral data to predict the percentage
 233 of insect lipids added to mixtures of vegetable and seed oils are summarized in Table 1 and
 234 represented in Figure 5. To enhance prediction quality, specific wavenumbers identified through
 235 PCA loadings were selected rather than using the entire spectral range. This approach helps remove
 236 variables that might be irrelevant, noisy, or otherwise unreliable in the context of interest (Leardi
 237 and Nørgaard, 2004). For FT-MIR models, wavenumber regions between 3100–2600 cm⁻¹ and
 238 1850–650 cm⁻¹ were used, while the 6100–4000 cm⁻¹ range was chosen for FT-NIR PLSR models.
 239 PLSR models used 7 factors to explain most of the relevant variance in the training set while
 240 minimizing the standard error of cross-validation (SE_{CV}). A leave-one-out cross-validation
 241 approach was employed to prevent overfitting by mitigating the impact of random noise (Ayvaz *et*
 242 *al.*, 2016). The correlation coefficients of cross-validation were 0.99 and the SE_{CV} values ranged
 243 from 1.15 to 2.21% (w/w). An external validation set was used to validate the models, and the
 244 results followed the same trend of the cross-validation, obtaining SE_P values lower than 2.32% and
 245 good correlation (R_P>0.99). The predictive qualities of the models were reported based on the RPD
 246 values An RPD above 3 indicates suitability for routine analysis, while values above 5 reflect a
 247 reliable model for quality control and an RPD greater than 8 indicates excellent predictive
 248 capability. The best predictive ability was obtained for PLSR models with FT- MIR with a RPD
 249 value of 18.32.

250 **Table 1.** Performance statistics of calibration and external validation models developed to quantify
 251 insect lipid content based on MIR and NIR data.

Device	Range (cm ⁻¹)	N _{cv}	Factors	R _{CV}	SE _{CV}	N _P	R _P	SE _P	RPD
MIR (Agilent Cary 630)	3100-2600; 1850-650	106	7	0.99	1.15	40	0.99	1.21	18.32
NIR (NeoSpectra Scanner)	6100-4000	103	7	0.99	2.21	37	0.99	2.32	9.23

252 Abbreviations used: N_{cv}: number of samples in the calibration set; R_{cv}: correlation coefficient of
 253 cross-validation; SE_{cv}: standard error of cross-validation; N_p: number of samples in the validation
 254 set; R_p: correlation coefficient of validation; SE_p: standard error of validation; RPD: Ratio of
 255 performance to deviation.

256 Our results are in line with those of other authors who have quantified a specific oil in a blend.
 257 Mendes *et al.* (2015) quantified soybean oil in a mixture with olive oil by NIR and MIR
 258 spectroscopy in the same range as our study. They reported a good correlation to predict the content
 259 of soybean oil in the blend but had higher SEP = 4.89 % when using MIR spectral data. Du *et al.*
 260 (2021) also quantified by NIR the camellia oil mixed with corn, rapeseed, and sunflower oil,
 261 achieving SEP from 2.17 to 3.19%.

262 *Fatty acid profile*

263 The fatty acid profile of *A. domesticus*, *L. migratoria*, olive, linseed, avocado, almond, and
 264 sunflower oil are shown in Table 2. The most common FA were palmitic (C16:0, 37.86%), stearic
 265 (C18:0, 10.43%), oleic (C18:1n9, 20.50%) and linoleic (C18:2n6, 27.08%) for *A. domesticus* and
 266 palmitic (35.19%), stearic (9.98%), oleic (25.94%), linoleic (17.84%) and α -linolenic (C18:3n3,
 267 8.45%) for *L. migratoria*. These FA were the 95.87 and 97.4% % of the total FA content,
 268 respectively. Our results are in agreement with previous studies performed with *A. domesticus* and
 269 *L. migratoria* (Egonyu *et al.*, 2021; Orkusz *et al.*, 2023; Osimani *et al.*, 2017). Olive and almond
 270 oils had high oleic acid content 69.29% and 66.06%, respectively, while avocado oil was notably
 271 rich in palmitic acid (22.84%). Sunflower oil contains a significant amount of linoleic acid
 272 (54.67%), an omega-6 (n6) fatty acid, whereas linseed has high α -linolenic acid content (45.37%),
 273 an omega-3 (n3) fatty acid. The individual fatty acids were classified into saturated FA (SFA),
 274 unsaturated FA (UFA), monounsaturated FA (MUFA), and polyunsaturated FA (PUFA) based on
 275 the structure of their lipid chains. Significant differences in the distribution of SFA and UFA were
 276 observed between vegetable and insect lipids. Vegetable and seed oils had a higher percentage of
 277 UFA (76.32- 87.49%). The FA of the insects was approximately equally divided between SFA
 278 (47.03-49.48%) and UFA (50.52-52.97%). In terms of UFA content, the

279 **Table 2.** Fatty acid composition (%) of vegetable, seed oils and insect lipids.

Fatty acids (%)	<i>A. domesticus</i>	<i>L. migratoria</i>	Linseed	Avocado	Olive	Almond	Sunflower
C12:0	0.10±0.02 ^a	0.26±0.03 ^b	0	0	0	0.06±0.01 ^a	0
C14:0	0.76±0.01 ^a	1.60±0.14 ^b	0.08±0.01 ^c	0.07±0.02 ^c	0.04±0.02 ^d	0.13±0.01 ^c	0.18±0.01 ^c
C16:0	37.86±0.15 ^a	35.19±1.07 ^b	8.97±0.23 ^c	22.84±0.23 ^d	15.24±0.04 ^c	9.79±0.61 ^c	9.26±0.07 ^c
C16:1 n9	0.27±0.02 ^a	0	0	0	0.08±0.03 ^b	0	0
C16:1 n7	0.55±0.07 ^{a,c}	0.73±0.13 ^a	0.07±0.01 ^b	9.17±0.04 ^c	0.72±0.06 ^a	0.46±0.00 ^c	0
C18:0	10.43±0.28 ^a	9.98±0.50 ^a	4.60±0.09 ^b	0.77±0.03 ^c	2.81±0.18 ^d	2.53±0.12 ^{d,e}	3.62±0.05 ^{d,f}
C18:1 n9	20.50±0.32 ^a	25.94±0.51 ^b	23.34±0.14 ^c	48.67±0.22 ^d	69.29±0.03 ^e	66.06±0.12 ^f	30.40±0.00 ^g
C18:1 n7	0.92±0.07 ^a	0	1.15±0.18 ^a	7.82±0.04 ^b	3.88±0.30 ^c	3.15±0.54 ^c	1.87±0.25 ^a
C18:2 n6	27.08±0.01 ^a	17.84±0.19 ^b	16.19±0.04 ^c	10.21±0.10 ^d	7.03±0.05 ^e	17.82±0.05 ^b	54.67±0.28 ^f
C18:3 n3	1.20±0.06 ^a	8.45±0.11 ^b	45.37±0.03 ^c	0.45±0.04 ^d	0.52±0.09 ^d	0	0
C20:0	0.33±0.01 ^a	0	0.13±0.05 ^a	0	0.26±0.12 ^a	0	0
C20:1 n9	0	0	0.09±0.00 ^a	0	0.13±0.02 ^a	0	0
SFA	49.48±0.43 ^a	47.03±0.46 ^b	13.78±0.39 ^c	23.68±0.28 ^d	18.35±0.11 ^e	12.51±0.71 ^c	13.06±0.03 ^c

UFA	50.52±0.43 ^a	52.97±0.46 ^b	86.22±0.39 ^c	76.32±0.28 ^d	81.65±0.11 ^e	87.49±0.71 ^c	86.94±0.03 ^c
MUFA	22.24±0.48 ^a	26.68±0.38 ^b	24.66±0.32 ^c	65.66±0.22 ^d	74.11±0.16 ^e	69.67±0.66 ^f	32.27±0.25 ^g
PUFA	28.29±0.05 ^a	26.29±0.09 ^b	61.56±0.07 ^c	10.66±0.06 ^d	7.54±0.04 ^e	17.82±0.05 ^f	54.67±0.28 ^g
n-6	27.08±0.01 ^a	17.84±0.19 ^b	16.19±0.04 ^c	10.21±0.10 ^d	7.03±0.05 ^e	17.82±0.05 ^b	54.67±0.28 ^f
n-3	1.20±0.06 ^a	8.45±0.11 ^b	45.37±0.03 ^c	0.45±0.04 ^d	0.52±0.09 ^d	0	0

280 Results are expressed as mean ± standard deviation. Different letters are significantly different
 281 (Tukey test, $p < 0.05$) in each row.

282 *L. migratoria* was divided in half for MUFA (26.68%) and PUFA (26.29%). While the *A.*
 283 *domesticus* had values more balanced toward the PUFA (28.29%), mainly due to the content of
 284 linoleic acid. *A. domesticus* and *L. migratoria* lipids were combined with all vegetable oils,
 285 resulting in samples with diverse fatty acid profiles, shown in Supplementary Table S3. The
 286 samples formulated with olive, almond, and avocado oils were richer in MUFA due to their high
 287 oleic acid content. In contrast, samples with higher amounts of sunflower and linseed oils had a
 288 higher percentage of PUFA, as they contribute linoleic and α -linolenic acid, respectively. Samples
 289 with a greater proportion of insect lipids had a more balanced composition, with insect lipids being
 290 the primary contributors to SFA.

291 *PLSR models to predict SFA, MUFA, and PUFA*

292 SFA, MUFA, and PUFA values were selected to create the prediction models, whereas UFA was
 293 discarded because of their roundness, and the n6 and n3 values were excluded because they did not
 294 differ from the linoleic and α -linolenic acid values, respectively. The statistical performance of the
 295 PLSR models developed is summarized in Table 3. The listed values include the data from both
 296 cross-validation and external validation, with the number of samples used varying between models
 297 due to the removal of samples with high leverage or residuals (Aykas *et al.*, 2020). To enhance the
 298 prediction quality, models were developed with the selected regions of the spectrum, focusing on
 299 characteristic lipid bands and removing infrared signals with irrelevant or noisy information. The
 300 number of factors selected was determined by minimizing SE_{cv} and R_{cv} values (factors < 10), with
 301 7 or 8 factors used during calibration to prevent under- or over-fitting the models. The PLSR
 302 models in this study showed a strong correlation ($0.987 \leq R_{cv} \leq 0.999$) and low error ($0.24\% \leq$
 303 $SE_{cv} \leq 2.21\%$) in the prediction of SFA, MUFA, and PUFA. Notably, models generated from
 304 spectra collected by the portable MIR spectrometer exhibited the best predictive performance, with
 305 lower error and higher correlation coefficients. The PLSR model performance was also evaluated
 306 using the external validation set, revealing similar performance across models in terms of error
 307 (SE_{cv} and SE_p) and correlation coefficient (R_{cv} and R_p). The SE_p values ranged from 0.30 to 0-
 308 54% for the three fatty acids groups in MIR validation models and ranged from 1.41 to 3.85% for
 309 NIR external validation models. Higher performance was observed with MIR compared to NIR,
 310 with RPD values based on MIR data exceeding 8, indicating excellent prediction, while NIR-based
 311 RPD values exceeded 3.1, making them suitable for screening or even quality control, particularly
 312 for SFA results. In both cases, SFA prediction showed better accuracy compared to MUFA and
 313 PUFA predictions. The predicted values from MIR and NIR for cross-validation and external
 314 validation are shown in Figure 6 and Figure 7, respectively. The regression line demonstrates how
 315 well the regression aligns with the best possible slope (slope=1) represented by the dotted line, with
 316 none of the predicted parameters deviating significantly from optimal. Additionally, it is possible
 317 to observe that the entire range included in the model is well-represented by the samples.

318 **Table 3.** Statistical performance of calibration and external validation models developed for
 319 predicting SFA, MUFA, and PUFA content based on MIR and NIR data.

		Range cal.	N _{cv}	F	R _{cv}	SE _{cv}	Range val.	N _p	R _p	SE _p	RPD
SFA	MIR	12.51-49.48	105	8	0.999	0.24	19.46-48.97	39	0.999	0.30	28.8
	NIR	12.51-49.48	88	7	0.993	1.26	19.46-48.97	40	0.989	1.41	6.2
MUFA	MIR	22.24-74.11	100	8	0.999	0.66	22.75-64.50	39	0.999	0.50	26.1
	NIR	22.24-74.11	84	7	0.987	2.21	22.75-64.50	40	0.965	3.40	3.7
PUFA	MIR	7.54-61.56	102	8	0.999	0.68	11.34-54.74	39	0.999	0.54	22.7
	NIR	7.54-61.56	80	8	0.992	1.49	11.34-54.74	40	0.955	3.85	3.1

320 Abbreviations used: N_{cv}: number of samples in the calibration set; F: number of factors; R_{cv}:
 321 correlation coefficient of cross-validation; SE_{cv}: standard error of cross-validation; N_p: number of
 322 samples in the validation set; R_p: correlation coefficient of validation; SE_p: standard error of
 323 validation; RPD: Ratio of performance to deviation.

324 *PLSR models to predict fatty acid content*

325 A total of 12 fatty acids were detected in the vegetable oils and insect lipids, with six selected to
 326 build PLSR prediction models. These fatty acids were chosen due to their high variability and
 327 prominence in insect lipids. The selected fatty acids were myristic (0.04–1.60%), palmitic (8.97–
 328 37.86%), stearic (0.77–10.43%), oleic (20.50–69.29%), linoleic (7.03–54.67%), and α -linolenic
 329 (0.00–45.37%). The remaining fatty acids almost overlap the minimum and the maximum values.
 330 The statistics of PLSR performance of each device for each parameter are summarized in Table 4
 331 and represented in Figure 8 and Figure 9. The prediction models were developed following the
 332 same guidelines as the previous ones and using a limited spectral range focused on the lipid region.
 333 The plot of reference values versus those predicted by the PLSR models shows that the samples
 334 are well-distributed across the whole range, except in the case of α -linolenic acid. The highest
 335 contribution of α -linolenic acid was from linseed oil, which had a content 5.4 times higher than *L.*
 336 *migratoria* and 37.8 times higher than *A. domesticus*. Not in such a perfect way, this distribution
 337 can be also observed in the case of linoleic acid, with sunflower oil and *A. domesticus* being the
 338 two major contributors. Overall, the PLSR models based on the spectra collected by the portable
 339 MIR device showed greater predictive capabilities compared to the handheld NIR spectrometer,
 340 following the performance of both devices in predicting SFA, MUFA, and PUFA. The correlation
 341 coefficient achieved during the calibration (R_{cv}) was over 0.995 for all the variables and the errors
 342 (SE_{cv}) ranged from 0.04 to 0.87%. The models were applied to predict values from the external
 343 validation set and evaluate its predictive performance. The SE_p (0.04 - 0.66%) had values around
 344 the corresponding SE_{cv} and also for the coefficients of correlation (R_p>0.994). Based on RPD
 345 values obtained from the validation set prediction (RPD > 8.2), the models demonstrated excellent
 346 predictive performance, reaching a value of 23.9 for oleic acid quantification. These MIR models
 347 demonstrated better performance for the prediction of the main FA composition than the results
 348 obtained by Liu *et al.* (2021). These authors analyzed 50 insect oil samples with a benchtop MIR
 349 spectrometer and created PLSR models to quantify 7 fatty acids that achieved SE_p value under
 350 4.87% but RPD values between 1.04 to 2.88. There are no other studies that analyze the lipid profile
 351 of insects based on mid-infrared spectra collected with a portable device with such variability, but

352 the results obtained can be compared with those obtained in oils of another origin. Plans *et al.*
 353 (2015) quantified levels of major FA in omega-3 oil dietary supplements of fish, cod liver, and
 354 flaxseed oil, samples rich in PUFA and n3, their sample set has higher variability in these
 355 compounds. The PLSR models based on the MIR spectra obtained with a 5-bounce ZnSe crystal
 356 ATR accessory also showed robustness with a high correlation coefficient ($R_P \geq 0.93$), and SE_P
 357 between 0.53 and 2.13%. Salas-Valerio *et al.* (2022) analyzed a smaller sample set of butter and
 358 margarine, validation with an independent sample set showed errors below 2.4% and a high
 359 correlation with a single bounce device as used in this work. Using an accessory ATR crystal with
 360 a higher number of bounces (five) the results improved to errors below 2.0%.

361 The calibration results obtained by NIR were lower than those achieved by MIR analysis. However,
 362 NIR spectra showed SE_{CV} ranged from 0.04 and 2.74% and good linearity ($R_{CV} > 0.979$), except for
 363 linoleic acid, whose prediction was not as robust ($R_{CV} = 0.88$, $SE_P = 4.64\%$), it could be a problem of
 364 sampling as mentioned above. The results of the external validation show values similar to those
 365 obtained in the internal validation carried out using cross-validation. The RPD value was also
 366 calculated, and the results were above 3 for the prediction of the individual unsaturated fatty acid
 367 (myristic, palmitic, and stearic acids), and α -linolenic acid suggesting that the generated models
 368 could be successfully used for screening. In the case of myristic acid, the prediction by NIR is
 369 comparable to MIR, the errors and correlations are equal in both calibration and validation, and
 370 even the RPD value was higher for the PLSR algorithm-created NIR spectral data. These results
 371 indicate that the spectral information in the IR region can provide enough information to obtain the
 372 fatty acid profile. The PLSR NIR models built up in this study were comparable to those reported
 373 by Yao *et al.* (2020) and Salas-Valerio *et al.* (2022) for the prediction of individual FA using
 374 handheld NIR devices with the same technology, but with three tungsten lamps, specifically the
 375 NeoSpectra Micro device (Si-Ware Systems, Inc., Cairo, Egypt). Yao *et al.* (2020) reported SE_P
 376 ranging from 1.60 to 3.55% for the main FA present in chip frying oil, while Salas-Valerio *et al.*
 377 (2022) predicted the main FA in butter and margarine with RPD values ranging from 2.5 to 6. These
 378 findings are in line with the RPD values obtained in this study for the quantification of FA in insect
 379 lipid samples, which ranged from 2.3 to 9.0.

380 **Table 4.** Statistical performance of calibration and external validation models developed for fatty
 381 acids content based on MIR and NIR data.

		Range cal.	N_{CV}	F	R_{CV}	SE_{CV}	Range val.	N_P	R_P	SE_P	RPD
Myristic acid C14:0	MIR	0.04-1.60	102	6	0.995	0.04	0.20-1.43	39	0.994	0.04	8.2
	NIR	0.04-1.60	102	6	0.994	0.04	0.20-1.43	40	0.994	0.04	9.0
Palmitic acid C16:0	MIR	8.97-37.86	100	8	0.999	0.34	14.23-37.31	39	0.999	0.40	16.8
	NIR	8.97-37.86	88	7	0.993	0.97	14.23-37.31	40	0.976	1.68	4.1
Stearic acid C18:0	MIR	0.77-10.43	105	8	0.999	0.13	2.64-10.34	39	0.999	0.11	18.1
	NIR	0.77-10.43	87	6	0.996	0.19	2.64-10.34	40	0.971	0.41	4.5
Oleic acid C18:1 n9	MIR	20.50-69.29	102	8	0.999	0.67	21.10-60.51	39	0.999	0.49	23.9
	NIR	20.50-69.29	84	8	0.979	2.74	21.10-60.51	40	0.945	4.15	2.8
Linoleic acid	MIR	7.03-54.67	102	8	0.996	0.87	9.22-49.00	39	0.998	0.58	16.2

C18:2 n6	NIR	7.03-54.67	84	8	0.880	4.64	9.22-49.00	40	0.902	4.07	2.3
α-linolenic acid	MIR	0.00-45.37	99	7	0.997	0.73	0.25-37.96	39	0.998	0.66	14.8
C18:3 n3	NIR	0.00-45.37	82	9	0.984	1.97	0.25-37.96	40	0.980	2.07	4.8

382 Abbreviations used: N_{CV}: number of samples in the calibration set; F: number of factors; R_{CV}:
383 correlation coefficient of cross-validation; SE_{CV}: standard error of cross-validation; N_P: number of
384 samples in the validation set; R_P: correlation coefficient of validation; SE_P: standard error of
385 validation; RPD: Ratio of performance to deviation.

386 4. Conclusion

387 Portable MIR and handheld NIR spectroscopic spectrometers represent a reliable, cost-effective,
388 and rapid tool for quantifying insect lipids and determining their fatty acid profile *in situ*. Both
389 miniaturized devices successfully quantified the insect lipid content in oil mixtures, with a SE_P
390 below 2.21%, R_P higher than 0.99, and RPD values greater than 9.23. PLSR models developed
391 using both MIR and NIR spectral data demonstrated strong performance in predicting the SFA,
392 MUFA, and PUFA content, as well as individual fatty acids, in insect lipids and related samples.
393 Overall, the models based on MIR spectra exhibited superior predictive accuracy compared to those
394 from the portable NIR spectrometer, obtaining SE_P values ranging from 0.04% to 0.66% and RPD
395 values over 8.2. This method offers a promising alternative for farmers and the insect industry,
396 enabling rapid and accurate analysis of lipids with minimal sample amounts and no need for sample
397 pretreatment.

398

399 ORCID of Authors

400 C. Mendez-Sanchez 0000-0001-6843-3927; M. Keshani Ranasinghe 0000-0002-1792-83-10; C.
401 Güell 0000-0002-4566-5132; M. Ferrando 0000-0002-2076-4222; J.C. Domingo 0000-0002-6356-
402 0836; S. de Lamo Castellvi 0000-0002-5261-6806

403

404 References

405 Aguilar, J. G. D. S., 2021. An overview of lipids from insects. *Biocatalysis and Agricultural*
406 *Biotechnology* 33: 101967. <https://doi.org/10.1016/j.bcab.2021.101967>
407 Armenta, S., Garrigues, S., and De La Guardia, M., 2007. Determination of edible oil parameters
408 by near-infrared spectrometry. *Analytica Chimica Acta* 596(2): 330-337.
409 <https://doi.org/10.1016/j.aca.2007.06.028>
410 Arrese, E. L., and Soulages, J. L., 2010. Insect Fat Body: Energy, Metabolism, and Regulation.
411 *Annual Review of Entomology* 55(1): 207-225. <https://doi.org/10.1146/annurev-ento-112408-085356>
412 Aykas, D. P., Karaman, A. D., Keser, B., and Rodriguez-Saona, L., 2020. Non-Targeted
413 Authentication Approach for Extra Virgin Olive Oil. *Foods* 9(2): 221.
414 <https://doi.org/10.3390/foods9020221>
415 Aykas, D. P., and Rodriguez-Saona, L. E., 2016. Assessing potato chip oil quality using a portable
416 infrared spectrometer combined with pattern recognition analysis. *Analytical Methods* 8(4): 731-
417 741. <https://doi.org/10.1039/C5AY02387D>

419 Ayvaz, H., Sierra-Cadavid, A., Aykas, D. P., Mulqueeney, B., Sullivan, S., and Rodriguez-Saona,
420 L. E., 2016. Monitoring multicomponent quality traits in tomato juice using portable mid-infrared
421 (MIR) spectroscopy and multivariate analysis. *Food Control* 66: 79-86.
422 <https://doi.org/10.1016/j.foodcont.2016.01.031>

423 Benes, E., Biró, B., Fodor, M., and Gere, A., 2022. Analysis of wheat flour-insect powder mixtures
424 based on their near infrared spectra. *Food Chemistry: X* 13: 100266.
425 <https://doi.org/10.1016/j.fochx.2022.100266>

426 Birkel, E., and Rodriguez-Saona, L., 2011. Application of a Portable Handheld Infrared
427 Spectrometer for Quantitation of trans Fat in Edible Oils. *Journal of the American Oil Chemists'*
428 *Society* 88(10): 1477-1483. <https://doi.org/10.1007/s11746-011-1814-z>

429 Borghi, F. T., Santos, P. C., Santos, F. D., Nascimento, M. H. C., Corrêa, T., Cesconetto, M., Pires,
430 A. A., Ribeiro, A. V. F. N., Lacerda, V., Romão, W., and Filgueiras, P. R., 2020. Quantification and
431 classification of vegetable oils in extra virgin olive oil samples using a portable near-infrared
432 spectrometer associated with chemometrics. *Microchemical Journal* 159: 105544.
433 <https://doi.org/10.1016/j.microc.2020.105544>

434 Carta, G., Murru, E., Banni, S., and Manca, C., 2017. Palmitic Acid: Physiological Role,
435 Metabolism and Nutritional Implications. *Frontiers in Physiology* 8: 902.
436 <https://doi.org/10.3389/fphys.2017.00902>

437 Cebi, N., Bekiroglu, H., Erarslan, A., and Rodriguez-Saona, L., 2023. Rapid Sensing: Hand-Held
438 and Portable FTIR Applications for On-Site Food Quality Control from Farm to Fork. *Molecules*
439 28(9): 3727. <https://doi.org/10.3390/molecules28093727>

440 Cheseto, X., Baleba, S. B. S., Tanga, C. M., Kelemu, S., and Torto, B., 2020. Chemistry and sensory
441 characterization of a bakery product prepared with oils from African edible insects. *Foods*, 9(6),
442 800. <https://doi.org/10.3390/foods9060800>

443 Christy, A. A., Kasemsumran, S., Du, Y., and Ozaki, Y., 2004. The Detection and Quantification of
444 Adulteration in Olive Oil by Near-Infrared Spectroscopy and Chemometrics. *Analytical Sciences*
445 20(6): 935-940. <https://doi.org/10.2116/analsci.20.935>

446 Delicato, C., Schouteten, J. J., Dewettinck, K., Gellynck, X., and Tzompa-Sosa, D. A., 2020.
447 Consumers' perception of bakery products with insect fat as partial butter replacement. *Food*
448 *Quality and Preference*, 79, 103755. <https://doi.org/10.1016/j.foodqual.2019.103755>

449 Dossey, A. T., Tatum, J. T., and McGill, W. L., 2016. Modern Insect-Based Food Industry: Current
450 Status, Insect Processing Technology, and Recommendations Moving Forward. *En Insects as*
451 *Sustainable Food Ingredients*: 113-152. Elsevier. [https://doi.org/10.1016/B978-0-12-802856-](https://doi.org/10.1016/B978-0-12-802856-8.00005-3)
452 [8.00005-3](https://doi.org/10.1016/B978-0-12-802856-8.00005-3)

453 Du, Q., Zhu, M., Shi, T., Luo, X., Gan, B., Tang, L., and Chen, Y., 2021. Adulteration detection
454 of corn oil, rapeseed oil and sunflower oil in camellia oil by in situ diffuse reflectance near-infrared
455 spectroscopy and chemometrics. *Food Control* 121: 107577.
456 <https://doi.org/10.1016/j.foodcont.2020.107577>

457 Egonyu, J. P., Subramanian, S., Tanga, C. M., Dubois, T., Ekesi, S., and Kelemu, S., 2021. Global
458 overview of locusts as food, feed and other uses. *Global Food Security* 31: 100574.
459 <https://doi.org/10.1016/j.gfs.2021.100574>

460 Franco, A., Salvia, R., Scieuzo, C., Schmitt, E., Russo, A., and Falabella, P., 2021. Lipids from
461 Insects in Cosmetics and for Personal Care Products. *Insects* 13(1): 41.
462 <https://doi.org/10.3390/insects13010041>

463 Garrido-Varo, A., García-Olmo, J., and Pérez-Marin, M. D., 2015. Applications in Fats and Oils.
464 *En C. A. Roberts, J. Workman, and J. B. Reeves (Eds.), Agronomy Monographs*, pp. 487-558.

465 American Society of Agronomy, Crop Science Society of America, Soil Science Society of
466 America. <https://doi.org/10.2134/agronmonogr44.c19>

467 Garrido-Varo, A., Sánchez, M.-T., De La Haba, M.-J., Torres, I., and Pérez-Marín, D., 2017. Fast,
468 Low-Cost and Non-Destructive Physico-Chemical Analysis of Virgin Olive Oils Using Near-
469 Infrared Reflectance Spectroscopy. *Sensors* 17(11): 2642. <https://doi.org/10.3390/s17112642>

470 Guillén, M. D., and Cabo, N., 2002. Fourier transform infrared spectra data versus peroxide and
471 anisidine values to determine oxidative stability of edible oils. *Food Chemistry* 77(4): 503-510.
472 [https://doi.org/10.1016/S0308-8146\(01\)00371-5](https://doi.org/10.1016/S0308-8146(01)00371-5)

473 Laroche, M., Perreault, V., Marciniak, A., Gravel, A., Chamberland, J., and Doyen, A., 2019.
474 Comparison of Conventional and Sustainable Lipid Extraction Methods for the Production of Oil
475 and Protein Isolate from Edible Insect Meal. *Foods* 8(11): 572.
476 <https://doi.org/10.3390/foods8110572>

477 Leardi, R., and Nørgaard, L., 2004. Sequential application of backward interval partial least squares
478 and genetic algorithms for the selection of relevant spectral regions. *Journal of Chemometrics*
479 18(11): 486-497. <https://doi.org/10.1002/cem.893>

480 Lepage, G., and Roy, C. C., 1986. Direct transesterification of all classes of lipids in a one-step
481 reaction. *Journal of Lipid Research* 27(1): 114-120. [https://doi.org/10.1016/S0022-2275\(20\)38861-1](https://doi.org/10.1016/S0022-2275(20)38861-1)

483 Lerma-García, M. J., Ramis-Ramos, G., Herrero-Martínez, J. M., and Simó-Alfonso, E. F., 2010.
484 Authentication of extra virgin olive oils by Fourier-transform infrared spectroscopy. *Food*
485 *Chemistry* 118(1): 78-83. <https://doi.org/10.1016/j.foodchem.2009.04.092>

486 Liu, Z., Rady, A., Wijewardane, N. K., Shan, Q., Chen, H., Yang, S., Li, J., and Li, M., 2021.
487 Fourier-transform infrared spectroscopy and machine learning to predict fatty acid content of nine
488 commercial insects. *Journal of Food Measurement and Characterization* 15(1): 953-960.
489 <https://doi.org/10.1007/s11694-020-00694-9>

490 Manzano-Agugliaro, F., Sanchez-Muros, M. J., Barroso, F. G., Martínez-Sánchez, A., Rojo, S.,
491 and Pérez-Bañón, C., 2012. Insects for biodiesel production. *Renewable and Sustainable Energy*
492 *Reviews* 16(6): 3744-3753. <https://doi.org/10.1016/j.rser.2012.03.017>

493 Mendes, T. O., Da Rocha, R. A., Porto, B. L. S., De Oliveira, M. A. L., Dos Anjos, V. D. C., and
494 Bell, M. J. V., 2015. Quantification of Extra-virgin Olive Oil Adulteration with Soybean Oil: A
495 Comparative Study of NIR, MIR, and Raman Spectroscopy Associated with Chemometric
496 Approaches. *Food Analytical Methods* 8(9): 2339-2346. <https://doi.org/10.1007/s12161-015-0121-y>

498 Okere, E. E., Arendse, E., Nieuwoudt, H., Perold, W. J., and Opara, U. L., 2022. Non-destructive
499 Evaluation of the Quality Characteristics of Pomegranate Kernel Oil by Fourier Transform Near-
500 Infrared and Mid-Infrared Spectroscopy. *Frontiers in Plant Science* 13: 867555.
501 <https://doi.org/10.3389/fpls.2022.867555>

502 Olsen, E. F., Rukke, E.-O., Egeland, B., and Isaksson, T., 2008. Determination of Omega-6 and
503 Omega-3 Fatty Acids in Pork Adipose Tissue with Nondestructive Raman and Fourier Transform
504 Infrared Spectroscopy. *Applied Spectroscopy* 62(9): 968-974.
505 <https://doi.org/10.1366/000370208785793371>

506 Oonincx, D. G. A. B., and Van Der Poel, A. F. B., 2011. Effects of diet on the chemical composition
507 of migratory locusts (*Locusta migratoria*). *Zoo Biology* 30(1): 9-16.
508 <https://doi.org/10.1002/zoo.20308>

509 Orkusz, A., Dymińska, L., Banaś, K., and Harasym, J., 2023. Chemical and Nutritional Fat Profile
510 of *Acheta domesticus*, *Gryllus bimaculatus*, *Tenebrio molitor* and *Rhynchophorus ferrugineus*.
511 *Foods* 13(1): 32. <https://doi.org/10.3390/foods13010032>

512 Osimani, A., Garofalo, C., Milanović, V., Taccari, M., Cardinali, F., Aquilanti, L., Pasquini, M.,
513 Mozzon, M., Raffaelli, N., Ruschioni, S., Riolo, P., Isidoro, N., and Clementi, F., 2017. Insight into
514 the proximate composition and microbial diversity of edible insects marketed in the European
515 Union. *European Food Research and Technology* 243(7): 1157-1171.
516 <https://doi.org/10.1007/s00217-016-2828-4>

517 Ozaki, Y., Huck, C. W., and Beć, K. B., 2018. Near-IR Spectroscopy and Its Applications. En
518 *Molecular and Laser Spectroscopy*, pp. 11-38. Elsevier. <https://doi.org/10.1016/B978-0-12-849883-5.00002-4>

520 Plans, M., Wenstrup, M. J., and Rodriguez-Saona, L. E., 2015. Application of Infrared
521 Spectroscopy for Characterization of Dietary Omega-3 Oil Supplements. *Journal of the American*
522 *Oil Chemists' Society* 92(7): 957-966. <https://doi.org/10.1007/s11746-015-2666-8>

523 Rabasco Alvarez, A. M., and González Rodríguez, M. L., 2000. Lipids in pharmaceutical and
524 cosmetic preparations. *Grasas y Aceites* 51(1-2): 74- 96. <https://doi.org/10.3989/gya.2000.v51.i1-2.409>

526 Rodriguez-Saona, L. E., Giusti, M. M., and Shotts, M., 2016. Advances in Infrared Spectroscopy
527 for Food Authenticity Testing. En *Advances in Food Authenticity Testing*, pp. 71-116. Elsevier.
528 <https://doi.org/10.1016/B978-0-08-100220-9.00004-7>

529 Rumpold, B. A., and Schlüter, O. K., 2013. Nutritional composition and safety aspects of edible
530 insects. *Molecular Nutrition and Food Research* 57(5): 802-823.
531 <https://doi.org/10.1002/mnfr.201200735>

532 Saeys, W., Mouazen, A. M., and Ramon, H., 2005. Potential for Onsite and Online Analysis of Pig
533 Manure using Visible and Near Infrared Reflectance Spectroscopy. *Biosystems Engineering* 91(4):
534 393-402. <https://doi.org/10.1016/j.biosystemseng.2005.05.001>

535 Salas-Valerio, W. F., Aykas, D. P., Hatta Sakoda, B. A., Ludeña-Urquiza, F. E., Ball, C., Plans, M.,
536 and Rodriguez-Saona, L., 2022. In-field screening of trans-fat levels using mid- and near-infrared
537 spectrometers for butters and margarines commercialized in the Peruvian market. *LWT* 157:
538 113074. <https://doi.org/10.1016/j.lwt.2022.113074>

539 Sales-Campos, H., Reis De Souza, P., Crema Peghini, B., Santana Da Silva, J., and Ribeiro
540 Cardoso, C., 2013. An Overview of the Modulatory Effects of Oleic Acid in Health and Disease.
541 *Mini Reviews in Medicinal Chemistry* 13(2): 201-210.
542 <https://doi.org/10.2174/138955713804805193>

543 Tzompa-Sosa, D. A., Dewettinck, K., Gellynck, X., and Schouteten, J. J., 2021a. Replacing
544 vegetable oil by insect oil in food products: Effect of deodorization on the sensory evaluation. *Food*
545 *Research International*, 141, 110140. <https://doi.org/10.1016/j.foodres.2021.110140>

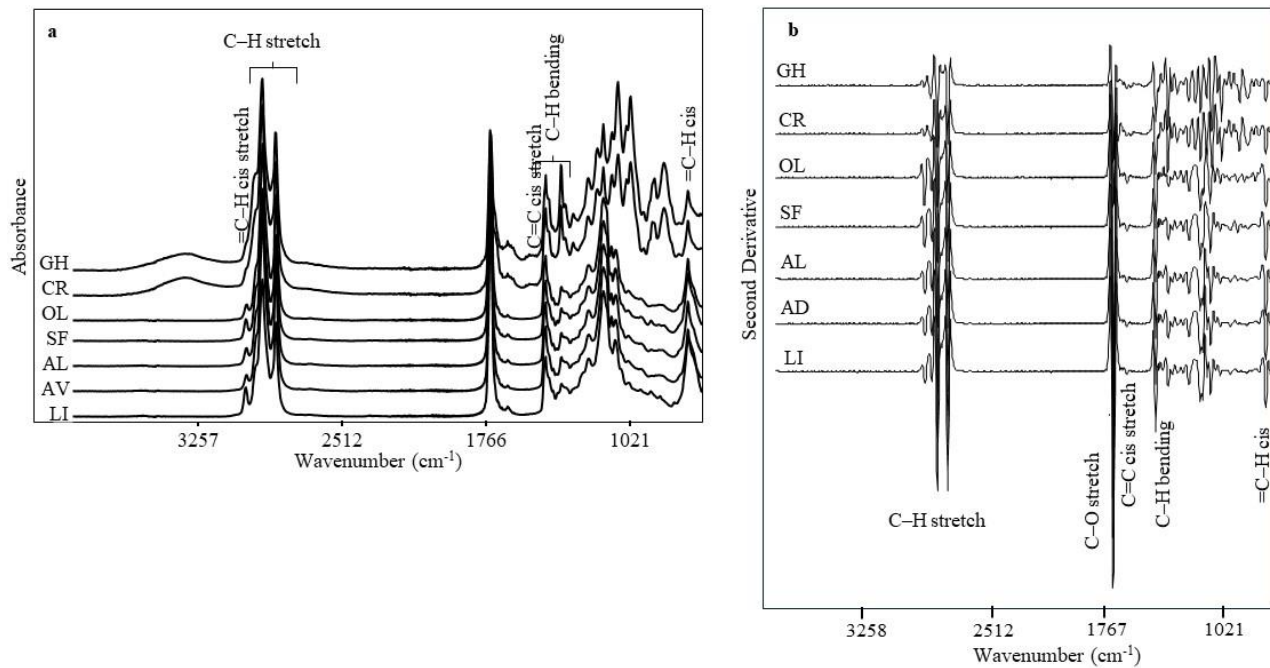
546 Tzompa-Sosa, D. A., Dewettinck, K., Provijn, P., Brouwers, J. F., De Meulenaer, B., and Oonincx,
547 D. G. A. B., 2021b. Lipidome of cricket species used as food. *Food Chemistry*, 349, 129077.
548 <https://doi.org/10.1016/j.foodchem.2021.129077>

549 Tzompa-Sosa, D. A., and Fogliano, V., 2017. Potential of Insect-Derived Ingredients for Food Applications. En V. D. C. Shields (Ed.), *Insect*
550 *Physiology and Ecology*. InTech. <https://doi.org/10.5772/67318>

551 Tarhan, İ., Ismail, A. A., and Kara, H., 2017. Quantitative determination of free fatty acids in extra
552 virgin olive oils by multivariate methods and Fourier transform infrared spectroscopy considering
553 different absorption modes. *International Journal of Food Properties* 20(sup1): S790-S797.
554 <https://doi.org/10.1080/10942912.2017.1312437>

555 Viola, P., and Viola, M., 2009. Virgin olive oil as a fundamental nutritional component and skin
556 protector. *Clinics in Dermatology* 27(2): 159-165.
557 <https://doi.org/10.1016/j.clindermatol.2008.01.008>

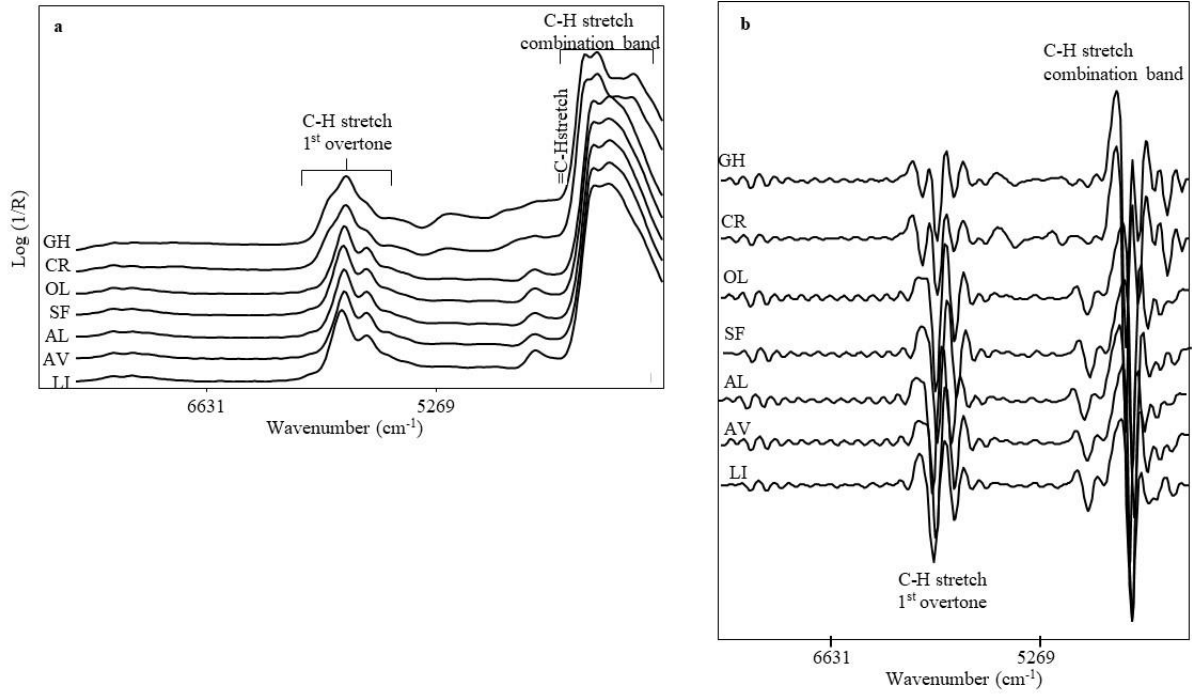
558 Wang, J., Ballon, A., Schroën, K., De Lamo-Castellví, S., Ferrando, M., and Güell, C., 2021.
559 Polyphenol Loaded W1/O/W2 Emulsions Stabilized with Lesser Mealworm (*Alphitobius*
560 *diaperinus*) Protein Concentrate Produced by Membrane Emulsification: Stability under Simulated
561 Storage, Process, and Digestion Conditions. *Foods* 10(12): 2997.
562 <https://doi.org/10.3390/foods10122997>
563 Yan, H., and Siesler, H. W., 2021. Applications of Handheld Near-Infrared Spectrometers. En R.
564 Crocombe, P. Leary, and B. Kammrath (Eds.), *Portable Spectroscopy and Spectrometry* (1.a ed.):
565 pp. 267-298. Wiley. <https://doi.org/10.1002/9781119636489.ch35>
566 Yao, S., Aykas, D. P., and Rodriguez-Saona, L., 2020. Rapid Authentication of Potato Chip Oil by
567 Vibrational Spectroscopy Combined with Pattern Recognition Analysis. *Foods* 10(1): 42.
568 <https://doi.org/10.3390/foods10010042>.
569



570
 571 **Figure 1.** Raw MIR spectral data (a) and (b) second derivative (17-point window size) of no mixed
 572 insect lipids and vegetable and seeds oils.

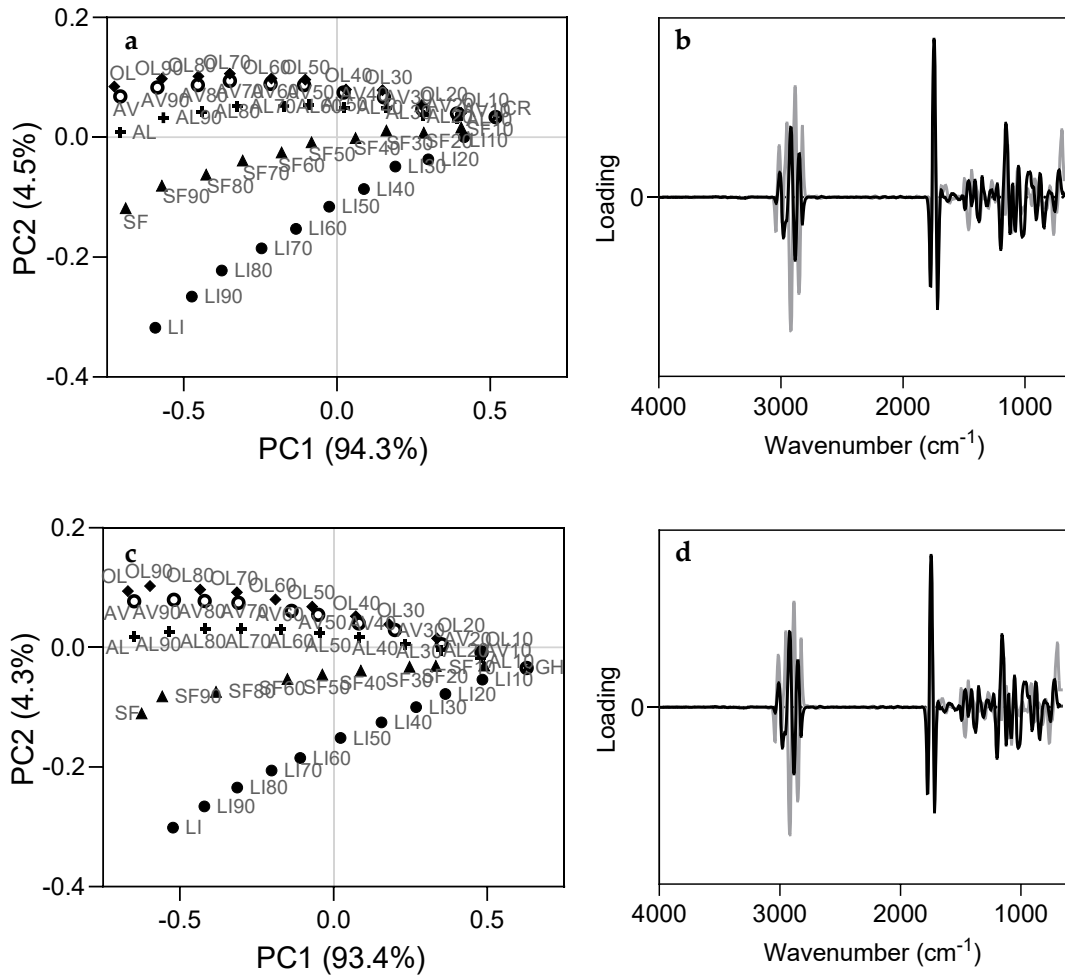
573

574
575

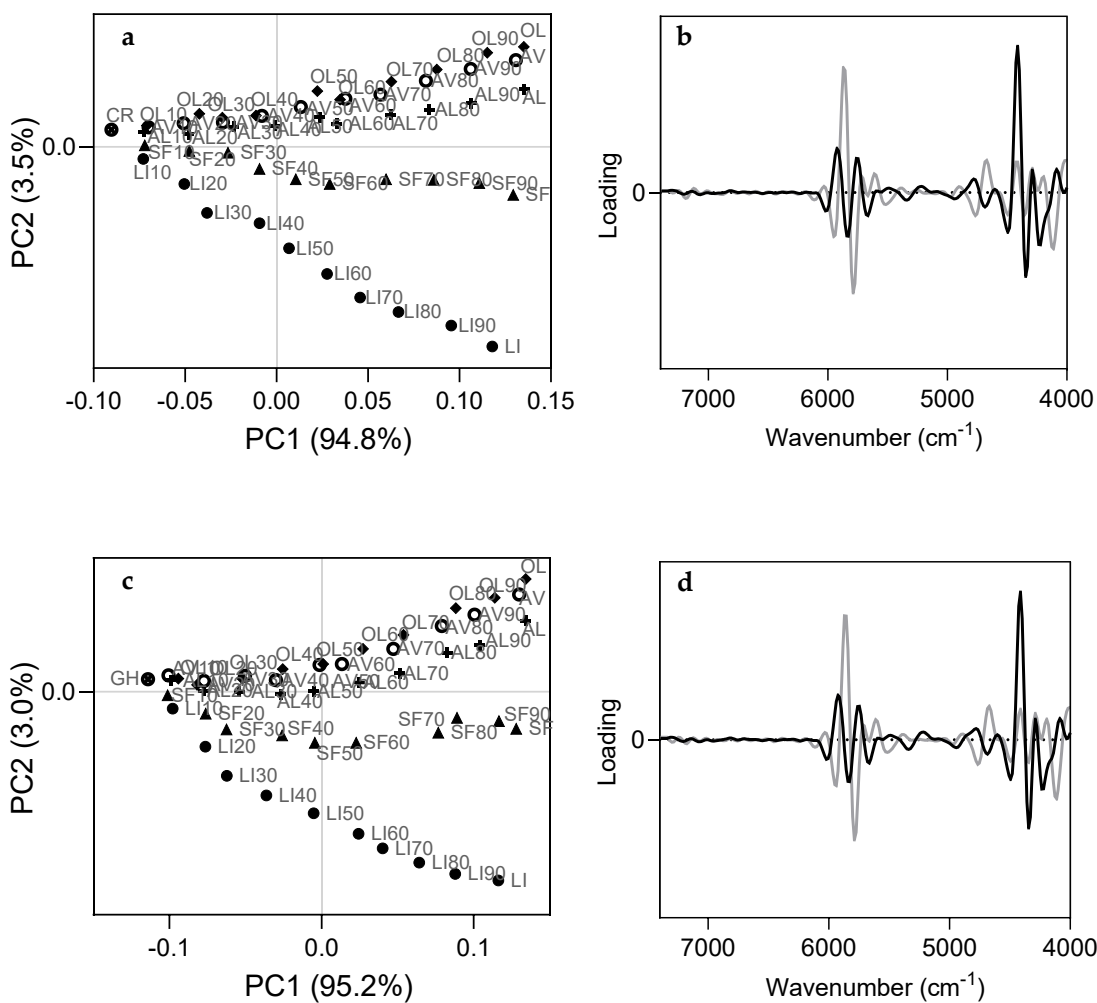


576
577
578
579
580
581

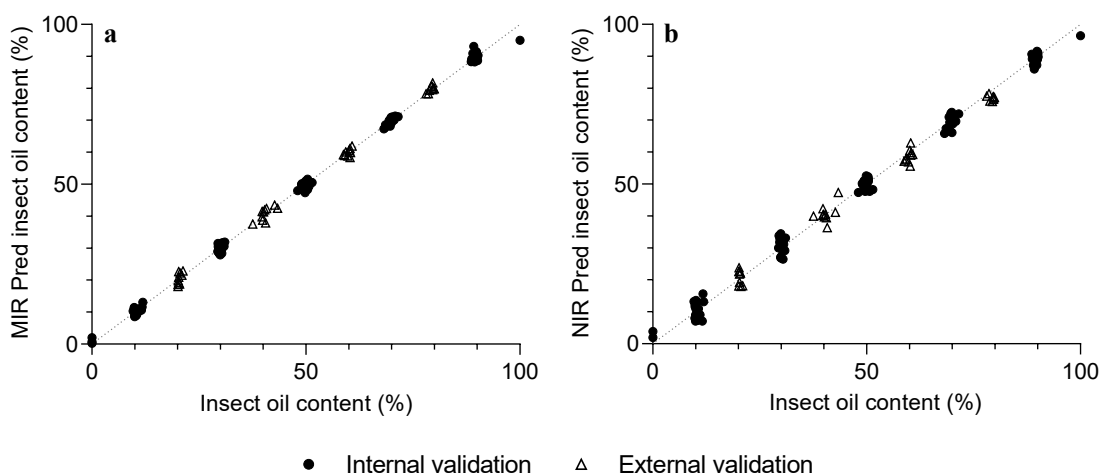
Figure 2. Raw NIR spectral data (a) and (b) second derivative (9-point window size) of no mixed insect lipids and vegetable and seeds oils



583
 584 **Figure 3.** PCA MIR plot of (a) *A. domesticus* and (c) *L. migratoria* and loadings of (b) *A.*
 585 *domesticus* and (d) *L. migratoria*. PC1: black; PC2: grey.
 586 Abbreviations used: LM: *L. migratoria*, AD: *A. domesticus*, OL: olive oil, SF: sunflower oil, AL:
 587 almond oil, AV: avocado oil, LI: linseed oil.



589
 590
 591
 592 **Figure 4.** PCA NIR plot of (a) *A. domesticus* and (c) *L. migratoria* and loadings of (b) *A.*
 593 *domesticus* and (d) *L. migratoria*. PC1: black; PC2: grey.
 594 Abbreviations used: LM: *L. migratoria*, AD: *A. domesticus*, OL: olive oil, SF: sunflower oil, AL:
 595 almond oil, AV: avocado oil, LI: linseed oil.

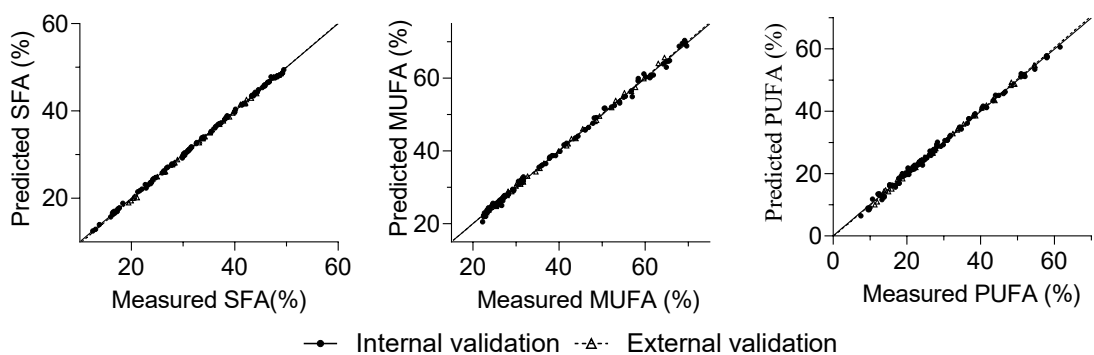


596

597 **Figure 5.** PLSR models calibration and validation plots for insect content prediction using (a) MIR
 598 and (b) NIR spectra.

599

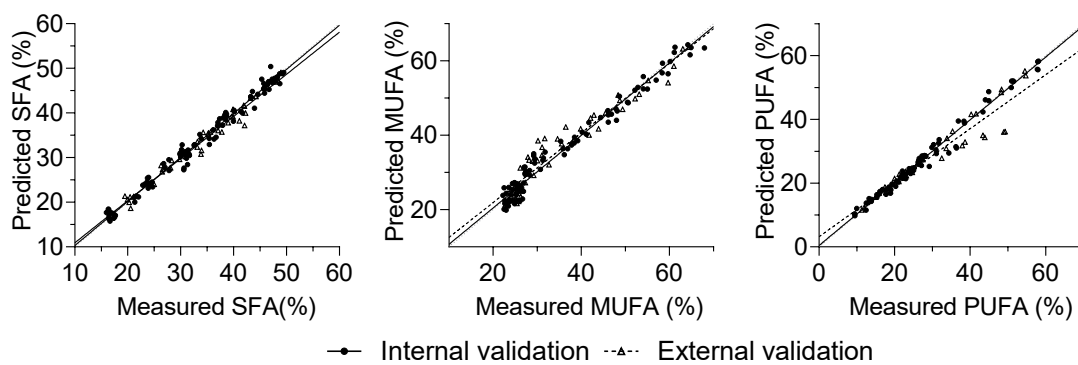
600



601

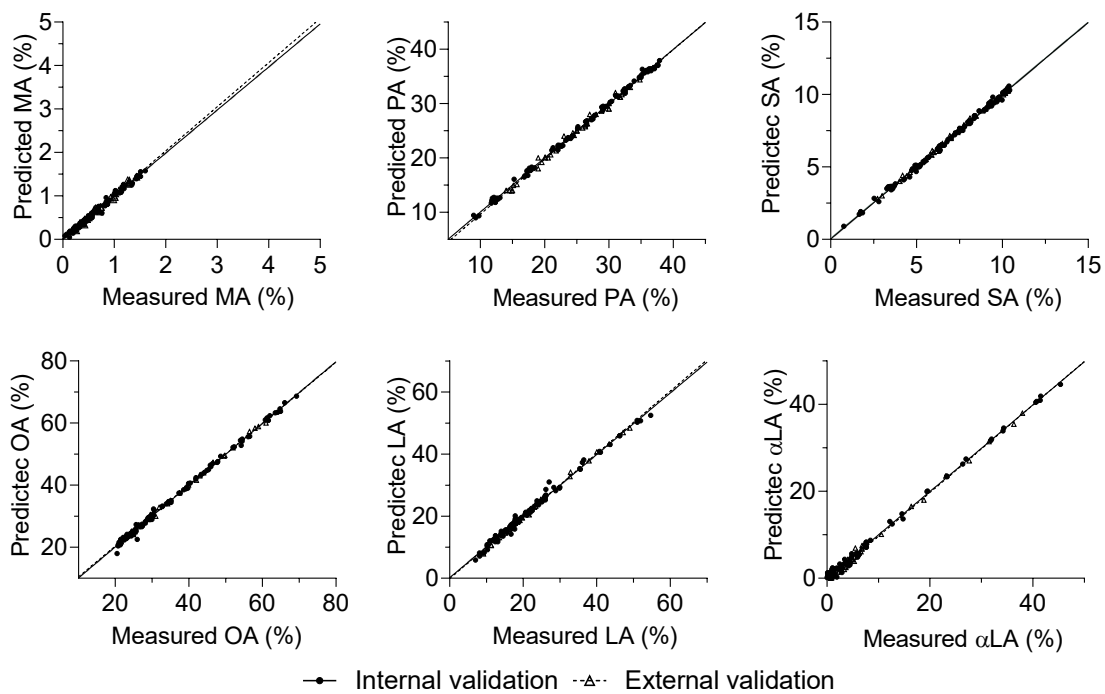
602 **Figure 6.** PLSR MIR models calibration and validation plots for SFA, MUFA, and PUFA
 603 quantification.

604



605
 606 **Figure 7.** PLSR NIR models calibration and validation plots for SFA, MUFA, and PUFA
 607 quantification.

608



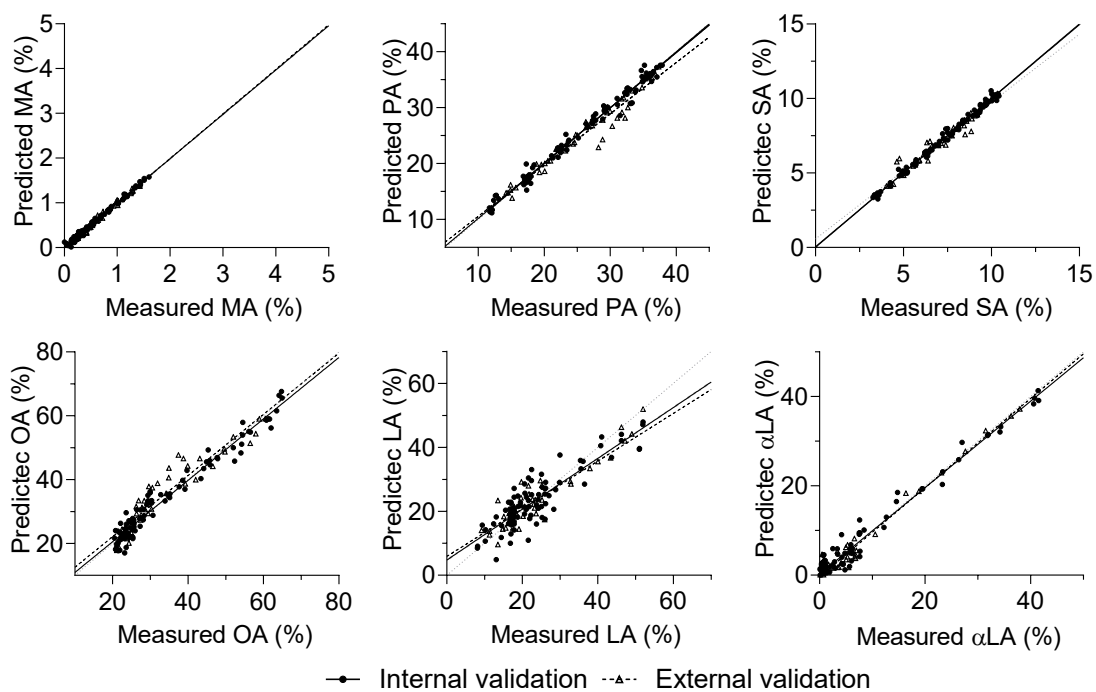
609

610 **Figure 8.** PLSR MIR models calibration and validation plots for fatty acid prediction.

611 Abbreviations used: MA: myristic acid; PA: palmitic acid; SA: stearic acid; OA: oleic acid; LA:

612 linoleic acid; α LA: α -linolenic acid.

613



614

615 **Figure 9.** PLSR NIR models calibration and validation plots for fatty acid prediction.

616 Abbreviations used: MA: myristic acid; PA: palmitic acid; SA: stearic acid; OA: oleic acid; LA:

617 linoleic acid; α LA: α -linolenic acid.

618

619

620 **Table S1.** The average oil content in blends of *A. domesticus* lipids with vegetable and seed oils is
 621 expressed as the percentage of insect lipids relative to the total weight of the sample.

<i>A. domesticus</i> (%)	Olive oil (%)	Sunflower oil (%)	Almond oil (%)	Avocado oil (%)	Linseed oil (%)
0.0 ± 0.0	100.0 ± 0.0	100.0 ± 0.0	100.0 ± 0.0	100.0 ± 0.0	100.0 ± 0.0
10.6 ± 0.7	88.8 ± 1.0	90.1 ± 0.2	89.0 ± 0.8	90.0 ± 0.1	89.3 ± 0.3
20.7 ± 0.0	78.7 ± 0.0	79.4 ± 0.0	79.0 ± 0.0	79.7 ± 0.0	79.5 ± 0.0
30.4 ± 0.4	69.7 ± 0.1	69.5 ± 0.1	69.5 ± 0.5	69.7 ± 1.1	69.5 ± 0.2
40.8 ± 0.0	59.6 ± 0.0	59.2 ± 0.0	57.3 ± 0.0	60.2 ± 0.0	59.9 ± 0.0
49.6 ± 0.7	50.5 ± 0.7	50.1 ± 0.6	51.1 ± 1.1	50.3 ± 1.0	50.0 ± 0.1
59.8 ± 0.0	39.8 ± 0.0	39.2 ± 0.0	41.2 ± 0.0	40.7 ± 0.0	39.9 ± 0.0
69.6 ± 0.6	30.1 ± 0.1	30.4 ± 0.3	30.2 ± 1.1	30.8 ± 0.8	30.5 ± 0.3
79.6 ± 0.0	20.1 ± 0.0	20.4 ± 0.0	20.0 ± 0.0	20.3 ± 0.0	21.2 ± 0.0
89.6 ± 0.5	10.0 ± 0.1	10.3 ± 0.3	10.6 ± 1.0	10.9 ± 0.2	10.4 ± 0.3
100.0 ± 0.0	0.0 ± 0.0	0.0 ± 0.0	0.0 ± 0.0	0.0 ± 0.0	0.0 ± 0.0

622
 623
 624
 625
 626
 627
 628
 629
 630
 631
 632
 633
 634
 635
 636
 637
 638
 639
 640
 641
 642
 643
 644

Table S2. The average oil content in blends of *L. migratoria* lipids with vegetable and seed oils is
 expressed as the percentage of insect lipids relative to the total weight of the sample.

<i>L. migratoria</i> (%)	Olive oil (%)	Sunflower oil (%)	Almond oil (%)	Avocado oil (%)	Linseed oil (%)
0.0 ± 0.0	100.0 ± 0.0	100.0 ± 0.0	100.0 ± 0.0	100.0 ± 0.0	100.0 ± 0.0
10.3 ± 0.6	89.7 ± 0.2	90.0 ± 0.1	89.5 ± 0.7	89.3 ± 1.5	89.5 ± 0.2
20.3 ± 0.0	79.7 ± 0.0	79.7 ± 0.0	79.9 ± 0.0	79.8 ± 0.0	79.9 ± 0.0
28.5 ± 0.4	70.1 ± 0.7	78.9 ± 0.2	70.3 ± 0.4	70.3 ± 0.1	69.9 ± 0.2
40.2 ± 0.0	60.1 ± 0.0	60.2 ± 0.0	59.4 ± 0.0	56.6 ± 0.0	62.4 ± 0.0
50.1 ± 0.6	50.4 ± 0.3	50.1 ± 0.7	49.4 ± 0.2	49.8 ± 0.2	49.4 ± 1.2
59.9 ± 0.0	39.7 ± 0.0	40.9 ± 0.0	40.2 ± 0.0	39.6 ± 0.0	39.7 ± 0.0
69.8 ± 0.9	31.1 ± 0.9	29.1 ± 0.9	30.3 ± 1.7	30.2 ± 0.2	29.9 ± 0.1
79.2 ± 0.0	20.7 ± 0.0	21.9 ± 0.0	20.6 ± 0.0	20.4 ± 0.0	21.4 ± 0.0
89.3 ± 0.5	10.8 ± 0.1	10.0 ± 0.3	10.9 ± 0.2	10.9 ± 0.7	10.8 ± 0.9
100.0 ± 0.0	0.0 ± 0.0	0.0 ± 0.0	0.0 ± 0.0	0.0 ± 0.0	0.0 ± 0.0

647

648

649 **Table S3.** The average SFA, MUFA, and PUFA content in blends of *A. domesticus* and *L.*
650 *migratoria* lipids with vegetable and seed oils included in the calibration set. The values are
651 expressed as a percentage of the total sample weight. The label number indicate the vegetable oil
652 percentage.

	<i>A. domesticus</i>			<i>L. migratoria</i>		
	SFA	MUFA	PUFA	SFA	MUFA	PUFA
Sunflower 90%	16.64	31.28	52.08	16.45	31.71	51.84
Sunflower 70%	24.16	29.21	46.63	23.33	30.58	46.09
Sunflower 50%	31.09	27.30	41.61	30.19	29.45	40.36
Sunflower 30%	38.34	25.31	36.36	36.90	28.34	34.75
Sunflower 10%	45.67	23.29	31.05	43.70	27.23	29.08
Olive 90%	22.05	67.93	10.01	21.24	69.32	9.44
Olive 70%	27.76	58.42	13.82	26.78	60.17	13.05
Olive 50%	33.91	48.17	17.91	32.64	50.48	16.88
Olive 30%	40.14	37.79	22.06	38.28	41.15	20.57
Olive 10%	46.38	27.39	26.22	43.90	31.85	24.25
Avocado 90%	26.24	61.36	12.41	25.93	61.90	12.17
Avocado 70%	31.29	52.85	15.86	30.61	54.09	15.30
Avocado 50%	36.32	44.39	19.29	35.38	46.13	18.49
Avocado 30%	41.68	35.36	22.96	40.01	38.39	21.60
Avocado 10%	46.64	27.01	26.35	44.38	31.09	24.52
Linseed 90%	17.51	24.40	58.08	17.33	24.87	57.80
Linseed 70%	24.60	23.92	51.48	23.85	25.27	50.88
Linseed 50%	31.64	23.45	44.91	30.89	25.70	43.41
Linseed 30%	38.52	22.98	38.50	37.06	26.07	36.87
Linseed 10%	45.85	22.48	31.67	43.65	26.47	29.87
Almond 90%	16.79	64.18	19.03	16.32	64.92	18.76
Almond 70%	23.92	55.03	21.05	22.68	57.00	20.32
Almond 50%	30.86	46.12	23.02	30.01	47.87	22.12
Almond 30%	38.62	36.17	25.21	36.16	40.21	23.63
Almond 10%	45.31	27.58	27.11	43.32	31.29	25.38

653

654

655